Microscopic theory of successive phase transitions in alkali metal cyanides

A. F. Sadreev and Yu. V. Sukhinin

L. V. Kirenski Institute of Physics, Siberian Branch of the Academy of Sciences of the USSR, Krasnoyarsk

(Submitted 14 April 1989; resubmitted 25 July 1989)
Zh. Eksp. Teor. Fiz. **97**, 283–301 (January 1990)

The energy levels and the wave eigenfunctions of the cyanogen groups are found using a cubic potential with eight minima. These eigenfunctions are employed to obtain a finite-dimensional representation of the Hubbard operators which describe the interaction of cyanogen groups with one another and also the interaction of these groups with elastic strains. The latter interaction is shown to be responsible for two high-temperature first-order phase transitions: from the cubic O_h^5 $(z=1)$ phase to the trigonal D_{2h}^{17} $(z=1)$ phase, and then to the orthorhombic D_{2h}^{25} $(z=1)$ phase with the appropriate quadrupole ordering of the cyanogen group. These phase transitions are accompanied by distortions of the cyanogen-group potentials. In particular, in the rhombic phase the potential can have two or four minima in the equilibrium orientation of the cyanogen groups along the [110] axis. It is shown that further cooling results in antiferromagnetic ordering of the dipole interactions of the cyanide groups. A specific example of KCN is considered.

1. INTRODUCTION

It is well known that ferroelectrics with a one-particle two-minimum (two-well) potential, such as KH_2PO_4, $NaNO_2$, etc., are described satisfactorily by the pseudospin formalism.[1,2] In fact, if the wells are sufficiently deep, we can ignore vibrations of particles inside each well and consider the two lowest states split by the tunneling. These two states make it possible to represent the interactions between the particles as of the spin–spin type. However, there is an enormous number of crystals in which phase transitions involve ordering of rigid molecular groups that rotate in multiminima potentials. In this case the description requires a large number of quantum states $|a\rangle$ of a molecule. Therefore, instead of the Pauli matrices it is necessary to use other operators. The Hubbard operators[3] are most convenient for this purpose and nowadays they are being used successfully in describing quantum magnetic materials with an arbitrary spin and an arbitrary anisotropy.[4,5]

The principal feature of such a description of the rotatable molecules is that the symmetry of the system is used during the initial stage because the eigenstates of a molecule considered allowing for the crystal potential can be classified in accordance with the irreducible representations of the symmetry group G of a crystal.[6] The interactions between the molecules can also be described using the same symmetry classification of the eigenstates, so that there is no difficulty in identifying the interactions responsible for spontaneous symmetry breaking, because it is accompanied by mixing of the states of the irreducible representation G.

We shall apply this approach to alkali-metal cyanides. These compounds were selected for two reasons. Firstly, the mobile molecular cyanogen groups CN are the simplest, which helps in solving the quantum-mechanical problem, but on the other hand their phase diagrams are quite complex. Secondly, a microscopic theory of alkali metal cyanides is available[7-10] and this theory describes the CN groups by spherical harmonics. We shall use this theory in the present treatment.

2. SELECTION OF THE HAMILTONIAN

We shall describe a sequence of phase transitions by defining the Hamiltonian of a crystal and its initial high-temperature cubic phase O_h^5 in which an MCN crystal (where M = K, Na, or Rb) has a structure similar to NaCl. It is shown in Fig. 1 that each cyanogen group is in a potential formed by the short-range interactions of atoms in this group, with the octahedral environment consisting of six M^+ ions in the first coordination sphere. This interaction will be approximated by the repulsive Born–Mayer potential

$$V_{i\mu}=C_1\sum_{\sigma=\pm1}\exp\{-C_2|\mathbf{x}_{i\mu}+\sigma h\mathbf{z}|\},\qquad(1)$$

where $\mathbf{x}_{i\mu}=\mathbf{x}_i+\mathbf{x}_\mu$; $\mathbf{x}_i$ are the instantaneous positions of the center of mass of the ith cyanogen group; $\mathbf{x}_\mu$ is the position of the μth M^+ ion; $\mathbf{z}=(\sin\theta\cos\varphi,\sin\theta\sin\varphi,\cos\theta)$ is a unit vector defining the cyanogen group orientation.

The lattice degrees of freedom and the lattice instability of the phase transition can be allowed for by expanding the distances in terms of elastic strains (see Ref. 11):

$$|\mathbf{x}_\mu+\sigma h\mathbf{z}|\approx|\mathbf{R}_\mu+\sigma h\mathbf{z}|+u_{\alpha\beta}R_\mu^\alpha(R_\mu^\beta+\sigma h z^\beta),\qquad(2)$$

where R_μ are the equilibrium states between the cyanogen groups and the M^+ ions. Substituting Eq. (2) into Eq. (1) and expanding in terms of $u_{\alpha\beta}$, we find that the cyanogen group potential has two components. The first is governed

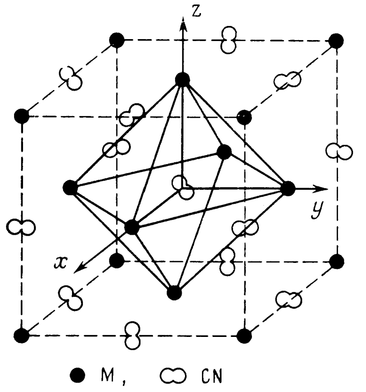

FIG. 1. Cubic phase of KCN with the NaCl structure. The continuous lines define the octahedron formed by the nearest-neighbor K^+ ions. The coordinate axes x, y, and z coincide with the crystallographic axes.

0038-5646/90/010160-11$03.00

by the equilibrium distances between the cyanogen groups and the M^+ ions and depends only on $\mathbf{z}$, so that it governs the orientational potential of the cyanogen group

$$U(\theta,\varphi)=C_1\sum_{\mu=1}^{6}\sum_{\sigma=\pm1}\exp\{-C_2|\mathbf{R}_\mu+\sigma h\mathbf{z}|\}$$

$$=\alpha_0+\alpha_4K_4(\theta,\varphi)+\alpha_6K_6(\theta,\varphi), \tag{3}$$

where

$$\alpha_m=C_1\sum_{\mu=1}^{6}\sum_{\sigma=\pm1}\int d\Omega\exp\{-C_2|\mathbf{R}_\mu+\sigma h\mathbf{z}|\}K_m(\Omega). \tag{4}$$

The second component of the potential describes the interaction of the orientational degrees of freedom with elastic strains:

$$V=-C_1C_2\sum_{\mu=1}^{6}\sum_{\sigma=\pm1}\frac{R_\mu{}^\alpha(R_\mu{}^\beta+\sigma hz^\beta)}{|\mathbf{R}_\mu+\sigma h\mathbf{z}|}\exp\{-C_2|\mathbf{R}_\mu+\sigma h\mathbf{z}|\}u_{\alpha\beta}. \tag{5}$$

Now, using Eq. (3), we can write down the Hamiltonian of the cyanogen group in the form

$$H_R=\sum_{f=1}^{N}\{\hat{\mathbf{L}}_f{}^2/2I+U(\theta,\varphi)\}, \tag{6}$$

where I is the moment of inertia of the cyanogen group amounting to 1.48×10^{-39} g·cm² and $\hat{\mathbf{L}}$ is the angular momentum of the cyanogen group. The eigenfunctions of (6) are $|\mu_r\rangle$ and belong to the same energy level E_r^0 and are characterized by an irreducible representation.[6] Therefore,

$$H_R=\sum_r\sum_{\mu_r}\sum_{f=1}^{N}E_r{}^0\hat{X}_f^{\mu_r\mu_r}, \tag{7}$$

where r labels the irreducible representations G. Among the irreducible representations of the O_h group there are the one-dimensional A_{1g} A_{2u}, A'_{1g}, and A'_{2u}, the two-dimensional E_g and E'_g, and the three-dimensional F_{1u}, F_{2g}, F'_{1u}, and F'_{2g}, representations.[6]

We must now write down the specific potential of Eq. (3) for the cyanogen group in order to obtain the wave functions and then to find the matrix elements of the interactions. We shall begin with KCN. The constants C_1 and C_2 can be obtained from the expressions given in Ref. 12:

$$C_1=(A_{CC}A_{KK})^{1/2},\quad C_2={}^1/_2(a_{CC}+a_{KK}),$$

where, according to Refs. 13 and 14, we have

$$A_{KK}=1.07\cdot10^{-9}\text{ erg},\ A_{CC}=4.42\cdot10^{-9}\text{ erg},$$
$$a_{KK}=2.8\ \text{Å}^{-1},\quad a_{CC}=3.6\ \text{Å}^{-1}.$$

Consequently, we obtain $C_1=2.17\times10^{-9}$ erg and $C_2=3.2$ Å^{-1}. Moreover, in the case of KCN we know that the dumbbell length is $2h=1.17$ Å and that the distance a between the center of mass of the cyanogen group and the M^+ ion is 3.25 Å (Ref. 15). Substituting all these values into Eq. (4), we obtain

$$U(\theta,\ \varphi)=V_0[K_4(\theta,\ \varphi)+0.03K_6(\theta,\ \varphi)], \tag{8}$$
$$V_0=1.62\cdot10^{-13}\text{ erg},$$

where

$$K_4=({}^7/_{12})^{1/2}[Y_{40}+({}^5/_{14})^{1/2}(Y_{44}+Y_{4-4})], \tag{9}$$
$$K_6=({}^1/_8)^{1/2}[Y_{60}-({}^7/_2)^{1/2}(Y_{64}+Y_{6-4})].$$

The potential of Eq. (3) has eight minima directed along the four principal diagonals of a cube (Fig. 1), i.e., along the $\langle111\rangle$ axes:

$$\sin^2\theta={}^2/_3,\quad \varphi=\pm\pi/4+\pi n,\quad n=0,\ 1. \tag{10}$$

The height of the potential barrier is

$$\frac{5}{48}\left(\frac{21}{\pi}\right)^{1/2}V_0=4.4\cdot10^{-14}\text{ erg}.$$

The energy levels of the wave eigenfunctions of the cyanogen group were found by the variational Rayleigh-Ritz method.[16] The results obtained for the potential of Eq. (8) are presented in Table I.

Using the wave functions from this table and applying the selection rules to the matrix elements of the polar vector and to the tensor of rank 2 for the point symmetry O_h (Ref. 6), we can express the interaction (5) in terms of the Hubbard operators

$$V=\sum_{i=1}^{N}\langle\mu|V_{\alpha\beta}|\nu\rangle\hat{X}_i{}^{\mu\nu}u_{\alpha\beta}, \tag{11}$$

where

$$\langle\mu|V_{\alpha\beta}|\nu\rangle=-C_1C_2\sum_a\sum_{\sigma=\pm1}\int d\Omega\psi_\mu(\theta,\varphi)$$
$$\times\exp\{-C_2|a+\sigma hz|\}\frac{a^\alpha(a^\beta+\sigma hz^\beta)}{|a+\sigma hz|}\psi_\nu(\theta,\varphi), \tag{12}$$

where a represents the distance to all six nearest neighbors of the cyanogen group and the integral with respect to Ω is taken over the directions of the cyanogen group specified by the vector $\mathbf{z}$.

It therefore follows that the initial Hamiltonian which can be used to consider high-temperature phase transitions becomes

$$H=H_{\text{el}}+V+H_R. \tag{13}$$

3. HIGH-TEMPERATURE PHASE TRANSITIONS

We shall now estimate the various interactions. First of all, we shall utilize the experimental observation that high-temperature phase transitions do not result in dipole ordering of the cyanogen groups. Consequently, at this stage the dipole–dipole interactions can be ignored. An estimate of the quadrupole interaction is of the following form[9]:

$$V_{QQ}\sim6e^2Q^2/25a^5,\quad Q=zh^2q_N,$$

where in the case of KCN the value of q_N varies from -0.2 to -0.95. Consequently, the maximum quadrupole interaction does not exceed 10 K. An estimate of the interaction of the cyanogen groups via the strain field obtained using $\lambda_2/$

TABLE I.

Представ-ление	Energy levels, 10^{-14} erg	Eigenvalues
A_{1g}	-4.57	$\psi_1 = 0.58\,Y_{00} - 0.59\,K_4 + 0.51\,K_6 + 0.15\,K_8 - 0.17\,K_{10}$
F_{1u}	-4.33	$\psi_{\left\{ 2 \atop 3 \right\}} = 0.62\,Y_{11\left\{ c \atop s \right\}} + 0.27\,Y_{31\left\{ c \atop s \right\}} \mp 0.37\,Y_{33\left\{ c \atop s \right\}} - 0.37\,Y_{51\left\{ c \atop s \right\}}$ $\mp 0.34\,Y_{53\left\{ c \atop s \right\}} - 0.21\,Y_{55\left\{ c \atop s \right\}} + 0.01\,Y_{71\left\{ c \atop s \right\}} \pm 0.11\,Y_{73\left\{ c \atop s \right\}}$ $+ 0.05\,Y_{75\left\{ c \atop s \right\}} \pm 0.08\,Y_{77\left\{ c \atop s \right\}};$ $\psi_4 = 0.62\,Y_{10} - 0.47\,Y_{30} - 0.15\,Y_{50} - 0.52\,Y_{54c} + 0.21\,Y_{70}$ $- 0.22\,Y_{74c}$
A_{1u}	-4.31	$\psi_5 = 0.93\,Y_{32s} - 0.27\,Y_{72s} - 0.25\,Y_{76s}$
F_{2g}	-3.97	$\psi_{\left\{ 6 \atop 7 \right\}} = 0.77\,Y_{21\left\{ c \atop s \right\}} - 0.18\,Y_{41\left\{ c \atop s \right\}} \mp 0.49\,Y_{43\left\{ c \atop s \right\}} - 0.21\,Y_{61\left\{ c \atop s \right\}}$ $\mp 0.10\,Y_{63\left\{ c \atop s \right\}} - 0.28\,Y_{65\left\{ c \atop s \right\}};$ $\psi_8 = 0.77\,Y_{22s} + 0.52\,Y_{42s} - 0.32\,Y_{62s} - 0.17\,Y_{66s}$
F_{1u}	-1.62	$\psi_9 = -0.32\,Y_{10} - 0.25\,Y_{30} + 0.67\,Y_{50} - 0.51\,Y_{54c} - 0.21\,Y_{70}$ $+ 0.29\,Y_{74c}$
		. . .

$$Y_{lmc} = (Y_{lm} + Y_{l-m})/2^{1/2}$$
$$Y_{lms} = -i\,(Y_{lm} - Y_{l-m})/2^{1/2}.$$

C^0_{44}, where in the case of KCN we have $C^0_{44} \approx 3.1 \times 10^{-12}$ erg, gives a value of the order of 200 K. Therefore, the mechanism of high-temperature phase interactions that results in the quadrupole ordering is the coupling of the cyanogen groups with the metal environment which in our treatment is regarded as the interaction of the Hubbard operators with elastic strains. This is in full agreement with the results reported in Refs. 7–10.

On this basis we shall simplify the Hamiltonian of Eq. (13) by ignoring the interactions between the variables $\hat{X}$ at different lattice sites. We can then take a trace of all the variables $\hat{X}$ and write down the free energy directly in terms of the variables $u_{\alpha\beta}$:

$$F(u_{\alpha\beta}) = {}^1/_2 C^0_{\alpha\beta\gamma\delta} u_{\alpha\beta} u_{\gamma\delta} - \rho kT \ln \mathrm{Tr} \exp[-\beta(H_R + V)], \qquad (14)$$

where ρ is the density of the cyanogen groups (number of these groups per unit volume). The calculation of the trace in Eq. (14) requires diagonalization of the multidimensional matrix $H_R + V$. Clearly, we can ignore the states which are weakly populated at temperatures close to the phase transition point (≈ 170 K). For this reason (see below) the energy levels E^0_5, ... and the corresponding states can be ignored. Consequently, the operator $H_R + V$ can be written in the representation of states from Table I, which has the following form:

$$\begin{array}{cccccccc}
\lambda_1 & 0 & 0 & 0 & 0 & g_1 u_{xy} & g_1 u_{xz} & g_1 u_{yz} \\
0 & \lambda_2 & \lambda u_{xy} & \lambda u_{xz} & g_2 u_{yz} & 0 & 0 & 0 \\
0 & \lambda u_{xy} & \lambda_3 & \lambda u_{yz} & g_2 u_{xz} & 0 & 0 & 0 \\
0 & \lambda u_{xz} & \lambda u_{yz} & \lambda_4 & g_2 u_{xy} & 0 & 0 & 0 \\
0 & g_2 u_{yz} & g_2 u_{xz} & g_2 u_{xy} & \lambda_5 & 0 & 0 & 0 \\
g_1 u_{xy} & 0 & 0 & 0 & 0 & \lambda_6 & g u_{yz} & g u_{xz} \\
g_1 u_{xz} & 0 & 0 & 0 & 0 & g u_{yz} & \lambda_7 & g u_{xy} \\
g_1 u_{yz} & 0 & 0 & 0 & 0 & g u_{xz} & g u_{xy} & \lambda_8 \\
A_{1g} & \multicolumn{3}{c}{\underbrace{\qquad\qquad\qquad}_{F_{1u}}} & A_{2u} & \multicolumn{3}{c}{\underbrace{\qquad\qquad\qquad}_{F_{2g}}}
\end{array}, \qquad (15)$$

where

$$\lambda_1 = E_1^0 + \gamma_1 u_{\alpha\alpha},$$
$$\lambda_2 = E_2^0 + (\gamma_2 - \gamma_3) u_{xx} + \gamma_3 u_{\alpha\alpha},$$
$$\lambda_3 = E_2^0 + (\gamma_2 - \gamma_3) u_{yy} + \gamma_3 u_{\alpha\alpha},$$
$$\lambda_4 = E_2^0 + (\gamma_2 - \gamma_3) u_{zz} + \gamma_3 u_{\alpha\alpha},$$
$$\lambda_5 = E_3^0 + \gamma_4 u_{\alpha\alpha},$$
$$\lambda_6 = E_4^0 + (\gamma_5 - \gamma_6) u_{xx} + \gamma_6 u_{\alpha\alpha},$$
$$\lambda_7 = E_4^0 + (\gamma_5 - \gamma_6) u_{yy} + \gamma_6 u_{\alpha\alpha},$$
$$\lambda_8 = E_4^0 + (\gamma_5 - \gamma_6) u_{zz} + \gamma_6 u_{\alpha\alpha}.$$

The coupling constants can be found numerically from Eq. (12) and for KCN they are (in units of 10^{-12} erg)

$$\begin{array}{ll}
\gamma_1 = -3.99 & \lambda = 0.350, \\
\gamma_2 = -4.12, & g = 0.322, \\
\gamma_3 = -3.92, & g_1 = 0.324, \\
\gamma_4 = -4.00, & g_2 = 0.329, \\
\gamma_5 = -3.84, & \gamma_6 = -3.97.
\end{array} \qquad (16)$$

We can find the trace in Eq. (14) if we obtain the eigenvalues of the matrix (15). This procedure and also the calculation of the free energy are given in the Appendix A. Moreover, in the same Appendix A it is shown that the critical variable for KCN is not $C_{11}-C_{12}$, but the elastic modulus C_{44}, in agreement with the observations reported in Refs. 15 and 17. Essentially this is a simple consequence of the circumstance that the "bare" elastic modulus C^0_{44} of alkali metal cyanides is considerably less than $C^0_{11}-C^0_{12}$.

It follows therefore that the high-temperature phase transitions can be described using a reduced thermodynamic potential which includes only the off-diagonal components of the strain tensor. Moreover, for simplicity, we shall consider only the reduced four-dimensional representation A_{1g}

$+F_{1u}$, which does not result in any qualitative changes. In the case of quantitative estimates of, for example, the transition temperatures, we can use the Appendix A. Consequently, instead of Eq. (A3), we have

$$F={}^1/_2\tau(x^2+y^2+z^2)+\gamma xyz+{}^1/_4\alpha(x^4+y^4+z^4)+{}^1/_2\delta(x^2y^2+y^2z^2+z^2x^2), \tag{17}$$

where

$$\begin{gathered} x=u_{xy},\ y=u_{xz},\ z=u_{yz}, \\ \tau=4C_{44}=4(C_{44}{}^0-2\lambda^2\beta/\rho), \\ \gamma=\overset{0}{C}_{456}-\beta^2\lambda^3f\rho=C_{456}, \\ \alpha=\overset{0}{C}_{4444}-\lambda^4\beta^3f\rho(1-6f)/3=C_{4444}, \\ \delta=\overset{0}{C}_{4455}-\lambda^4\beta^3f\rho(1-6f)/3=C_{4455}, \\ f=\{3+\exp[-\beta(E_2{}^0-E_1{}^0)]\}^{-1} \end{gathered} \tag{18}$$

where C^0_{456}, C^0_{4444}, and C^0_{4455} are the nonlinear elastic moduli[18] of the cubic phase.

It is clear from the notation used in Eq. (18) that cooling reverses the signs of all the constants in Eq. (17). However, since the elastic moduli of order n are usually always larger than the elastic moduli of order $n-1$, we need to consider only the change in the sign of C_{44}. Another feature of the thermodynamic potential of Eq. (17) is the presence of the cubic term γxyz, which gives rise to first-order phase transitions. A similar form of the thermodynamic potential is obtained also in Ref. 10, where the components of the quadrupole ordering of the cyanogen groups serve as the order parameter.

An analysis of the phase diagram generated by Eq. (17) can be found in the Appendix B. Here we shall simply give the temperatures of the first-order phase transitions from the cubic to the rhombohedral phase

$$T_1=T_0\left\{1+{}^1/_{18}\frac{\gamma^2}{(\alpha+2\delta)C_{44}{}^0}\right\} \tag{19}$$

and from the rhombohedral to the orthorhombic phase

$$T_2=T_0\left\{1-{}^1/_{16}\frac{\gamma^2}{(\alpha+2\delta)}\frac{2\xi-1}{(\xi-1)^2}\right\},\quad \xi=\left(\frac{\alpha+\delta}{2\alpha}\right)^{1/2}, \tag{20}$$

where

$$T_0=\frac{2\rho\lambda^2}{C_{44}{}^0}\frac{1}{3+\exp[-\beta_0(E_2{}^0-E_1{}^0)]}\approx\frac{\rho\lambda^2}{2C_{44}{}^0}. \tag{21}$$

Bearing in mind that $\gamma\ll\alpha,\delta$, we can see that the temperature range of existence of the orthorhombic phase is quite narrow.

The calorimetric and structural data on cyanides and hydrogen sulfides of alkali metals[19] show that KCN and NaCN exhibit a sequence of first-order phase transitions $(000)\to(xxx)\to(x00)$, whereas in the case of CsCN, NaSH, KSH, and RbSH, there is only one transition from the cubic to the rhombohedral phase. It therefore follows that the proposed theory is in agreement with the experimental results. The difference in the sequence of the phase transitions in the case of the above crystals is simply due to the inequality (B9) which can be checked experimentally.

In the case of KCN the usual cooling and heating of samples reveals just one phase transition from the cubic to the orthorhombic phase at $T=168.3$ K accompanied by a change in the entropy amounting to about $R\ln 4$ (Refs. 20 and 21). An intermediate phase has been detected in KCN as a result of complex cooling and heating cycles near the 168 K transition temperature.[20,22] According to Refs. 20–22, this intermediate phase is monoclinic [and can designated by (xxy) in our notation], whereas it follows from the present study that the cubic and orthorhombic phases are separated by a stable rhombohedral phase. In our opinion, this conflict can be resolved bearing in mind that all the high-temperature transitions are of the first order. Therefore, for heating to cause the orthorhombic $(x00)$ phase to change to the stable rhombohedral phase (xxx) by the formation of seeds, the crystal must pass through metastable states of the monoclinic (xxy) phase, where $y<x$. Bearing in mind that the temperature range of stability of the rhombohedral phase in KCN is narrow (≈ 5 K), it follows that this phase can be observed after a very long time or a large number of heating–cooling cycles. The intermediate rhombohedral phase has been observed experimentally[23] for KCN. In the case of NaCN the rhombohedral phase can be formed by quenching the cubic modification from 300 °C (Ref. 19).

An analysis of the phase diagram is made here in the mean-field approximation, because the equation of state (B1) corresponds to an estimate of the statistical integral by the steepest-descent method

$$Z=\int Du(x)\exp\{-\beta F(u_{\alpha\beta})\}.$$

Allowance for the mean-square fluctuations about the equilibrium positions makes it necessary to add the phonon contribution to the thermodynamic potential of Eq. (17):

$$-kT\ln\sum_k\omega_k(u_{\alpha\beta}{}^0), \tag{22}$$

which alters the phase diagram. In Eq. (22), ω_k stands for the frequencies governed by $u^0_{\alpha\beta}$, of the lattice vibrations about the equilibrium positions. However, since we are dealing with first-order phase transitions, we shall ignore a weak logarithmic dependence of ω_k on temperature and assume that the critical fluctuations cannot develop in the available time. This situation is typical of first-order structural phase transitions.

4. QUADRUPOLE ORDERING OF CYANOGEN GROUPS

In order to understand what happens to the crystal structure and to the orientation of the cyanogen groups in phase transitions, we consider a fragment of the crystal lattice of MCN. Figure 1 shows the crystal structure of the high-temperature cubic phase characterized by $u_{\alpha\beta}=0$. The M^+ ions form an fcc unit cell with the cyanogen groups located at the midpoints of the edges. Moreover, one cyanogen group is located at the center of the cube, i.e., the immediate environment of a cyanogen group is an octahedron of the M^+ ions. The preferred orientation of the cyanogen groups is along four main diagonals of the cubic cell (at least this is true of NaCN and KCN—see Refs. 10, 19, 24, and 25). The cyanogen groups have eight degenerate directions in the cubic phase. These directions are defined by the centers of the triangles of which the octahedron is composed and this is naturally due to the repulsive nature of the inter-

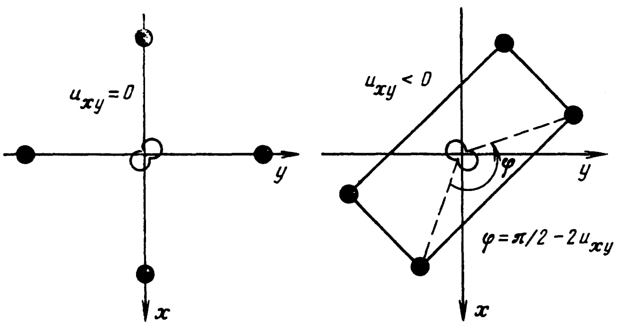

FIG. 2. Positions of the K^+ ions in the immediate environment of the cyanogen groups in the cubic and orthorhombic phases.

action of Eq. (1) between the M^+ ions and the cyanogen group atoms. The base of the cubic unit cell is deformed from a square into a rhomb with the angle $\varphi = \pi/2 - 2u_{xy}$, but the side walls of the cell are not affected (Fig. 2). Since in the $u_{xy} \neq 0$ phase the M^+ ions (or the cyanogen groups) can be used to construct a parallelepiped with its sides directed along the [110], [1$\bar{1}$0], and [001] axes, the (x00) phase is orthorhombic and its space symmetry group is D_{2h}^{25} (Ref. 26).

It therefore follows that the spontaneous strain u_{xy} can be used to identify a structural transition in an alkali metal cyanide crystal, whereas the ordering of the cyanogen groups is governed by the averages $\langle \hat{X}^{\mu\nu} \rangle$ which are related to the spontaneous strains in the crystal:

$$\lambda\rho\langle \hat{X}^{23}+\hat{X}^{32}\rangle = C_{44}{}^{0}u_{xy}. \tag{23}$$

This relationship is obtained from Eqs. (14) and (15) by differentiation with respect to u_{xy} using the reduced representation $A_{1g} + F_{1u}$. The averages are given by

$$\langle \hat{X}^{\alpha\beta}\rangle = Z^{-1}\sum_{\tilde{a}=1}^{4}\langle \tilde{a}\,|\,\hat{X}^{\alpha\beta}\,|\,\tilde{a}\rangle e^{-\beta E_{\tilde{a}}}, \quad Z=\sum_{\tilde{a}=1}^{4} e^{-\beta E_{\tilde{a}}}, \tag{24}$$

where $|\tilde{a}\rangle$ are the eigenstates of $H_R + V$, which for the orthorhombic phase are

$$\begin{aligned}
&|\tilde{1}\rangle = |1\rangle, && E_1 = E_1{}^0,\\
&|\tilde{2}\rangle = (|2\rangle - |3\rangle)/2^{1/2}, && E_2 = E_2{}^0 - \lambda u_{xy},\\
&|\tilde{3}\rangle = |4\rangle, && E_3 = E_2{}^0,\\
&|\tilde{4}\rangle = (|2\rangle + |3\rangle)/2^{1/2}, && E_4 = E_2{}^0 + \lambda u_{xy}.
\end{aligned} \tag{25}$$

Substituting Eq. (25) into Eq. (24) and then into Eq. (23), we readily obtain the self-consistency equation for the order parameter u_{xy} of the orthorhombic phase:

$$\frac{2\lambda\rho\,\mathrm{sh}\,(\beta\lambda u_{xy})}{1+2\,\mathrm{ch}\,(\beta\lambda u_{xy})+\exp[-\beta(E_2{}^0-E_1{}^0)]} = C_{44}{}^0 u_{xy}. \tag{26}$$

We can easily demonstrate that if $u_{xy} \to 0$, we formally obtain the temperature T_0 of a second-order phase transition given by Eq. (21).

Using Table I and Eq. (25) we readily obtain the average of any function of the angles:

$$\langle f(\theta,\varphi)\rangle = Z^{-1}\sum_{i=1}^{4}\int_0^{\pi} d\cos\theta \int_0^{2\pi} d\varphi f(\theta,\varphi)\,\tilde{\psi}_i^2(\theta,\varphi)\,e^{-\beta\tilde{E}_i}. \tag{27}$$

Hence, in particular, we find that the dipole moment of the cyanogen group in the orthorhombic phase is zero and the components of the quadrupole moment

$$Q_{\alpha\beta} = qh^2(3z_\alpha z_\beta - \delta_{\alpha\beta}), \tag{28}$$

where $z_1 = \sin\theta\cos\varphi$, $z_2 = \sin\theta\sin\varphi$, $z_3 = \cos\theta$, assume the following values

$$\begin{aligned}
&\langle Q_{xz}\rangle = \langle Q_{zy}\rangle = 0, \quad \langle Q_{\alpha\alpha}\rangle \sim u_{xy}{}^2,\\
&\langle Q_{xy}\rangle = \frac{1.8\,\mathrm{sh}\,(\beta\lambda u_{xy})\,h^2 q_N}{1+2\,\mathrm{ch}\,(\beta\lambda u_{xy})+\exp[-\beta(E_2{}^0-E_1{}^0)]},
\end{aligned} \tag{29}$$

where q_N is the effective charge. The values of the components of the quadrupole order parameter of Eq. (29) correspond to ordering of the cyanogen groups along the [110] axis.

We shall now consider the equilibrium orientations of the cyanogen groups in the orthorhombic phase. A spontaneous breaking of the cubic symmetry could occur because of the cooperative freezing of the cyanogen groups in one of the four equivalent directions.[27] However, numerous experimental results[10,19,24,25] demonstrate that the equilibrium orientations of the cyanogen groups change from the ⟨111⟩ directions in the cubic phase to ⟨110⟩ in the orthorhombic phase. One of the possible explanations of this change was put forward in Refs. 28 and 29. It is based on the assumption that the orientational potential of the cyanogen groups has local minima along the ⟨110⟩ directions, but the energy is higher than along ⟨111⟩. After transition to the orthorhombic phase the ⟨110⟩ directions become preferable from the energy point of view. We shall propose a different explanation based on the distortion of the metal octahedron (Fig. 1) at the phase transition because of the appearance of the terms with $u_{xy} \neq 0$. In general, both mechanisms of spontaneous reorientation of the equilibrium directions of the cyanogen groups are possible: those because of distortion of the immediate environment and those because of the existence of metastable minima in the potential described by Eq. (3), which in turn alters the orientational potential in the rhombic phase

$$V_{\mathrm{cub}}(\theta,\varphi) \to V_{\mathrm{orth}}(\theta,\varphi), \tag{30}$$

where according to Eq. (15) we have

$$\begin{aligned}
V_{\mathrm{orth}}(\theta,\varphi) &= V_{\mathrm{cub}}(\theta,\varphi) + 2\lambda u_{xy}\langle\theta,\varphi|\hat{X}^{23}+\hat{X}^{32}|\theta,\varphi\rangle\\
&= V_{\mathrm{cub}}(\theta,\varphi) + 2\lambda u_{xy}\psi_2(\theta,\varphi)\psi_3(\theta,\varphi).
\end{aligned} \tag{31}$$

In the leading order in respect of the angular functions, we have

$$V_{\mathrm{orth}}(\theta,\varphi) = 1.62V_0[\cos^4\theta + \sin^4\theta - {}^1/_2(\sin^2\theta\sin 2\varphi - 2\chi u_{xy})^2], \tag{32}$$

where according to Eq. (16) we find that $\chi = 0.08$ and $\lambda/V_0 = 1.36$. Minimization of Eq. (32) yields the equilibrium orientations of the cyanogen groups in the orthorhombic phase:

$$\varphi=\pi/4+\pi n,\quad n=0,1;\quad \sin^2\theta={}^2/_3(1+\chi u_{xy}),\quad 0<u_{xy}<\chi/2,$$

$$\varphi=\pi/4+\pi n,\quad \sin^2\theta=1,\quad u_{xy}>\chi/2. \tag{33}$$

It therefore follows that the spontaneous strain u_{xy} lifts the degeneracy in respect of the azimuthal angle φ, which can easily be understood from the figure and increases the polar angle θ. Within the framework of the reduced representation $A_{1g}+F_{1u}$ the value of χ is small, so that a fourfold degeneracy remains in the orthorhombic phase. Within the framework of the full eight-dimensional representation $A_{1g}+A_{2u}+F_{1u}+F_{2g}$ and subject to the appearance of the diagonal components $u_{\alpha\alpha}$ we can expect the rhombic phase to have the equilibrium direction $\sin^2\theta=1$, i.e., [110] (Ref. 30). It should be noted that the first solution of Eq. (33) again does not contradict the quadrupole ordering of the cyanogen groups of Eq. (29) along the [110] axis since degeneracy of the polar angle $\theta=\pm\sin^{-1}[(2/3)(1+\chi u_{xy})]^{1/2}$ gives $\langle\theta\rangle=0$ after thermodynamic averaging. The experimental data for KCN support the hypothesis of fourfold degeneracy, since the change in the entropy at the phase transition is less than R ln 4 (Ref. 19) and mean-square librations of the cyanogen groups in the orthorhombic phase are quite large ($\approx 24°$).[31]

We shall note one further disagreement between the experimentally observed pattern of the ordering of the cyanogen groups and our results. In our analysis these groups become ordered along the short side of the base (Fig. 3a), i.e., along the **a** axis, whereas in fact the ordering of the cyanogen groups in the orthorhombic phase of KCN occurs along the **b** axis,[32] i.e., parallel to the long side of the face in Fig. 3b. At first sight this is in conflict with the repulsive nature of the Born–Mayer interaction of Eq. (1) between the cyanogen groups and the M^+ ions. However, if we allow for the same interactions between the CN molecule at the center of the cube and the twelve CN molecules in the next coordination sphere, we find that the direction of the cyanogen groups in the orthorhombic phase changes by 90°. As shown in Fig. 3a, if the cyanogen groups had been ordered along the **a** axis, a strong repulsion would have been established between them.

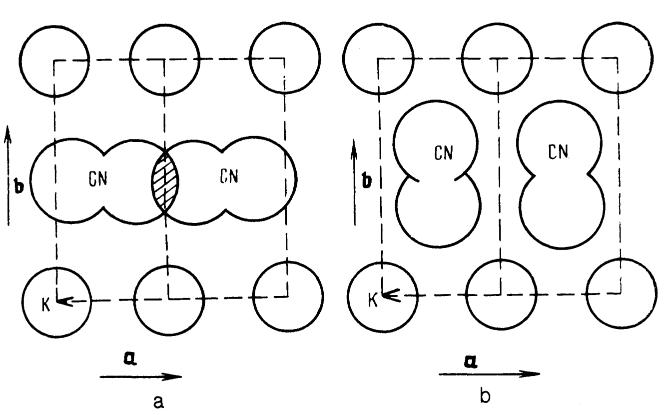

FIG. 3. a) Interaction of the cyanogen groups with the metallic environment determines the direction of the groups along the **a** axis. b) Interaction between the cyanogen groups described by the Born–Mayer potential results in ordering of these groups along the **b** axis.

In the rhombohedral phase (xxx) the distortion of the crystallographic structure caused by the fact that $|u_{xy}|=|u_{yx}|=|u_{xz}|$ represents compression of the lattice along one of the $\langle 111\rangle$ directions. Since the symmetry element (threefold axis) is conserved, the phase is clearly trigonal or rhombohedral.

On the basis of relationships of the (23) type, we can expect structural trigonal distortions to give rise to a quadrupole order parameter $\langle Q_{xy}\rangle=\langle Q_{xz}\rangle=\langle Q_{yz}\rangle$, which corresponds to ordering of the cyanogen groups along $\langle 111\rangle$. The selection of the ordering axis of the cyanogen groups is governed by the sign of $u_{\alpha\beta}$.

If we substitute the approximate values of $C_{44}^0=3.9\times10^{10}$ erg/cm^3 and $\rho=1.38\times10^{22}$ cm^{-3} into Eq. (21) allowing for Eq. (16), we find that to the phase transition temperature is $T\approx 50$ K. The discrepancy between this value and the experimental temperature 168 K is primarily due to reduction of the matrix of Eq. (15). In general, the temperatures of the high-temperature phase transitions are close to T_0, which can be found from the self-consistency equation for the orthorhombic phase, by analogy with Eq. (26). In the matrix (15) for this phase splits into four two-dimensional blocks

$$\begin{bmatrix} E_1{}^0 & g_1u_{xy}\\ g_1u_{xy} & E_2{}^0\end{bmatrix},\quad \begin{bmatrix} E_2{}^0 & \lambda u_{xy}\\ \lambda u_{xy} & E_2{}^0\end{bmatrix},$$

$$\begin{bmatrix} E_2{}^0 & g_2u_{xy}\\ g_2u_{xy} & E_3{}^0\end{bmatrix},\quad \begin{bmatrix} E_3{}^0 & gu_{xy}\\ gu_{xy} & E_3{}^0\end{bmatrix},$$

the eigenstates and eigenvalues of which are (if $u_{xy}>0$)

$$|\tilde{1}\rangle=\left(\frac{\eta+1}{2\eta}\right)^{1/2}|1\rangle-\left(\frac{\eta-1}{2\eta}\right)^{1/2}|5\rangle,\quad E_1={}^1/_2(E_1{}^0+E_3{}^0-\Delta_{31}\eta),$$

$$|\tilde{2}\rangle=(|2\rangle-|3\rangle)/2^{1/2},\quad E_2=E_2{}^0-\lambda u_{xy},$$

$$|\tilde{3}\rangle=\left(\frac{\varepsilon+1}{2\varepsilon}\right)^{1/2}|4\rangle-\left(\frac{\varepsilon-1}{2\varepsilon}\right)^{1/2}|8\rangle,\quad E_3={}^1/_2(E_2{}^0+E_4{}^0-\Delta_{42}\varepsilon),$$

$$|\tilde{4}\rangle=(|2\rangle+|3\rangle)/2^{1/2},\quad E_4=E_2{}^0+\lambda u_{xy}, \tag{34}$$

$$|\tilde{5}\rangle=(|6\rangle-|7\rangle)/2^{1/2},\quad E_5=E_3{}^0-gu_{xy},$$

$$|\tilde{6}\rangle=\left(\frac{\eta+1}{2\eta}\right)^{1/2}|5\rangle+\left(\frac{\eta-1}{2\eta}\right)^{1/2}|1\rangle,\quad E_6={}^1/_2(E_1{}^0+E_3{}^0+\Delta_{31}\eta),$$

$$|\tilde{7}\rangle=(|6\rangle+|7\rangle)/2^{1/2},\quad E_7=E_3{}^0+gu_{xy},$$

$$|\tilde{8}\rangle=\left(\frac{\varepsilon+1}{2\varepsilon}\right)^{1/2}|8\rangle+\left(\frac{\varepsilon-1}{2\varepsilon}\right)^{1/2}|4\rangle,\quad E_8={}^1/_2(E_2{}^0+E_4{}^0+\Delta_{42}\varepsilon),$$

where

$$\eta^2=1+4g_1{}^2u_{xy}{}^2/\Delta_{31}{}^2,\quad \varepsilon^2=1+4g_2{}^2u_{xy}{}^2/\Delta_{42}{}^2,$$

$$\Delta_{\alpha\beta}=E_\alpha{}^0-E_\beta{}^0.$$

The pattern of the energy level splitting in the orthorhombic phase is shown in Fig. 4.

Substituting Eq. (34) into Eqs. (24) and (23), we obtain the following self-consistency equation:

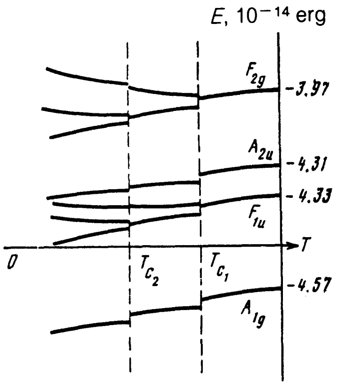

FIG. 4. Schematic representation of the splitting of the energy levels of the cyanogen groups in the rhombohedral and orthorhombic phases of KCN.

$$\begin{aligned}C_{44}{}^{0}\rho^{-1}u_{xy}=\Big[&\lambda e^{-\beta\Delta_{21}}\operatorname{sh}\beta\lambda u_{xy}\\&+ge^{-\beta\Delta_{31}}\operatorname{sh}\beta g u_{xy}\\&+\frac{2g_1{}^2u_{xy}}{\Delta_{31}\eta}e^{-\beta\Delta_{31}/2}\operatorname{sh}(\beta\Delta_{31}\eta/2)\\&+\frac{2g_2{}^2u_{xy}}{\Delta_{42}\varepsilon}e^{-\beta(\Delta_{21}+\Delta_{41})/2}.\\&\times\operatorname{sh}(\beta\Delta_{42}\varepsilon/2)\Big]\big[e^{-\beta\Delta_{21}}\operatorname{ch}\beta\lambda u_{xy}\\&+e^{-\beta\Delta_{31}}\operatorname{ch}\beta g u_{xy}+e^{-\beta\Delta_{31}/2}\operatorname{ch}(\beta\Delta_{31}\eta/2)\\&+e^{-\beta(\Delta_{21}+\Delta_{31})/2}\operatorname{ch}(\beta\Delta_{42}\varepsilon/2)\big]^{-1}.\end{aligned}\tag{35}$$

Hence we obtain the phase transition temperature given by Eq. (A5) in the Appendix A. Moreover, Eq. (35) allows us to estimate readily the maximum strain u_{xy} if we assume that $\tau=0$, which gives

$$u_{xy}\approx\rho g_1/C_{44}{}^{0}\approx0.09.\tag{36}$$

This estimate is in order-of-magnitude agreement with the results of x-ray structure investigations of the orthorhombic phase, which give $u_{xy}\approx0.15$ and $u_{xx}\approx0.05$ (Ref. 33).

5. DIPOLE ORDERING

The orthorhombic phase retains the head-tail symmetry of the cyanogen groups along the [110] axis. In the ground state this symmetry means that $\tilde{\psi}_1(\theta,\varphi)=\tilde{\psi}_1(\theta,\varphi+\pi)$. The dipole-dipole interaction is characterized by

$$V_{dd}=q_N{}^2\sum_{i,j}\left\{\frac{\mathbf{z}_i\mathbf{z}_j}{r_{ij}{}^3}-\frac{3(\mathbf{z}_i\mathbf{r}_{ij})(\mathbf{z}_j\mathbf{r}_{ij})}{r_{ij}{}^5}\right\},\tag{37}$$

where $\mathbf{z}=(\sin\theta\cos\varphi,\ \sin\theta\ \varphi,\ \cos\theta)$ and the summation carried out over the orthorhombic lattice sites occupied by the cyanogen groups mixes the states $|\tilde{1}\rangle$ and $|\tilde{2}\rangle$, $|\tilde{4}\rangle$, described by Eq. (34) and thus gives rise to a spontaneous polarization $\langle\mathbf{z}\rangle\neq0$. We shall now consider the hierarchy of the energy levels of Eq. (25) before the temperature of the transition to the dipole phase, which in the case of KCN amounts to 83 K (Ref. 34). If we use the estimate of Eq. (36) and the values of the constants of Eq. (16), we obtain (in units of 10^{-14} erg) that if $T\ll T_0$ then

$$\begin{aligned}&E_1=-7.43,\quad E_2=-6.64,\quad E_3=-5.46,\quad E_4=-2.24,\\&E_5=-7.22,\quad E_6=-1.44,\quad E_7=-1.02,\quad E_8=-2.98.\end{aligned}$$

Bearing in mind that the energy of the state $|\tilde{4}\rangle$ is considerably higher than E_1 and E_2, we can limit our treatment to just two states: $|\tilde{1}\rangle$ and $|\tilde{2}\rangle$. The state $|\tilde{5}\rangle$ is also close in energy to the ground state, but it does not become mixed with $|\tilde{1}\rangle$ by the dipole interactions. Then, the Hamiltonian of Eq. 37 assumes the following form in the representation of the $|\tilde{1}\rangle$ and $|\tilde{2}\rangle$ states:

$$\begin{aligned}V_{dd}=&-\frac{E_2-E_1}{2}\sum_{i=1}^{N}\sigma_i{}^z\\&+2q_N{}^2h^2D^2\sum_{i,j}^{N}\left(-\frac{3\sin^2\theta_{ij}\cos2\varphi_{ij}}{r_{ij}{}^3}\right)\sigma_i{}^x\sigma_j{}^x,\end{aligned}\tag{38}$$

where σ^α are the Pauli matrices,

$$D=\frac{1}{2^{1/2}}\left[\left(\frac{\eta+1}{2\eta}\right)^{1/2}\langle1|z_1|2\rangle+\left(\frac{\eta-1}{2\eta}\right)^{1/2}\langle3|z_1|5\rangle\right],$$

$$\langle i|z_1|j\rangle=\int d\Omega\psi_i\psi_j\sin\theta\cos\varphi.$$

The phase transition temperature and the spatial period of the dipole ordering can be found, as usual, from the equation

$$\chi^{-1}(\mathbf{q})=\chi_0{}^{-1}-V(\mathbf{q})=0,$$

or, according to Refs. 2 and 35, from

$$\omega_0\operatorname{cth}(\beta_c\omega_0)=\sum_{\mathbf{x}}V(\mathbf{x})e^{-i\mathbf{qx}},\tag{39}$$

where $V(\mathbf{x})$ is the dipole-dipole interaction of Eq. (38) and $\mathbf{x}$ represents all the vectors joining the CN groups. However, Eq. (39) can be used to find the nature of the ordering. We therefore have to turn to the equation of state considered in the mean-field approximation[35]

$$\xi_i=\sum_j V_{ij}\xi_j\frac{\operatorname{th}\beta\left[\omega_0{}^2+\left(\sum\limits_n V_{in}\xi_n\right)^2\right]^{1/2}}{\left[\omega_0{}^2+\left(\sum V_{in}\xi_n\right)^2\right]^{1/2}},\tag{40}$$

where $\xi_i=\langle\sigma_i^x\rangle$. The vicinity of the phase transition, where ξ_i are small, Eq. (40) simplifies to:

$$\hat{A}|\xi\rangle=|\xi\rangle,\quad A_{ij}=V_{ij}\omega_0{}^{-1}\operatorname{th}\beta\omega_0.\tag{41}$$

Equation (41) is a special case of

$$\hat{A}|\xi\rangle=\lambda|\xi\rangle.$$

The matrix $\hat{A}$ is diagonal in the q representation, so that the eigenvalues and the eigenstates are in each case characterized by the wave vector $\mathbf{q}$. A comparison of Eqs. (41) and (39) shows that the transition to the diagonal phase occurs when the smallest eigenvalue $\lambda(\mathbf{q}_0)$ becomes equal to 1 as a result of cooling. The structure of the dipole phase is therefore covered by the eigenvector $|\mathbf{q}_0\rangle$.

In general, it is not possible to solve Eq. (41). However, experiments showed that only doubling of the period occurs in the dipole phase. Then, the eigenvectors can be sought in the eight-dimensional representation where the variables ξ_1, ..., ξ_8 are located at eighth vertices of a primitive unit cell[37] shown in Fig. 5. According to Niemeyer,[37] the matrix elements A_{ij} are given by

$$A_{ii}=\sum_{n,m,l} V(2n\mathbf{a}+2m\mathbf{b}+2l\mathbf{c}),$$

$$A_{12}=A_{56}=A_{34}=A_{78}=\sum_{n,m,l} V[(2n+1)\mathbf{a}+2m\mathbf{b}+2l\mathbf{c}], \tag{42}$$

$$\cdots\cdots\cdots\cdots\cdots\cdots\cdots$$

$$A_{17}=A_{28}=\sum_{n,m,l} V[(2n+1)\mathbf{a}+(2m+1)\mathbf{b}+(2l+1)\mathbf{c}],$$

where *n*, *m*, and *l* are natural numbers.

If we consider a crystal KCN at $T=90$ K with the parameters[33] $|\mathbf{a}|=4.21$ Å, $|\mathbf{b}|=5.20$ Å, and $|\mathbf{c}|=6.11$ Å, we obtain the following numerical values of the matrix elements of Eq. (42):

j	1	2	3	4	5	6	7	8
A_{1j}	−0.17	4.99	−0.3	−2.04	−0.21	−0.21	−0.21	−0.21

Here, the unit length is $|\mathbf{c}_1|$.

The solution of Eq. (41) is equivalent to finding the minimum value of the quadratic form $\Sigma_{i,j}A_{ij}\xi_i\xi_j$, which in turn—as shown in Ref. 37—is equivalent to finding the minimum of the expression

$$\sum_j A_{ij}\varepsilon^{(\alpha)}_{P(i,j)}, \quad \alpha=1,\ldots,8, \tag{43}$$

where $\varepsilon^{(\alpha)}_{P(i,j)}$ are the eigenvalues of the operator representing the $i\leftrightarrow j$ transpositions of the cyanogen groups, as shown in Fig. 5. The eigenvectors and the eigenvalues of the transposition operator are given by Niemeyer in Ref. 37. Substituting the above data and the eigenvalues from Ref. 37 into Eq. (43), we can readily find a minimum for $\alpha=1,\ldots,8$. The ground state is doubly degenerate for $\alpha=3$ and 6. The corresponding eigenvectors form an ordered distribution of the dipoles shown in Fig. 6. The double degeneracy characterized by $\alpha=3$ and 6 is due to two orientations of the central dipole, which is quite evident from physical concentrations. Naturally, after the phase transition the dipoles are frozen in the configuration $|3\rangle$ or $|6\rangle$.

It is interesting to compare these results with those obtained by an analysis of the ground state of KCN at $T=0$ reported in Refs. 34 and 38–42. In Ref. 34 the ground state of the dipole system of KCN is derived by the approximate

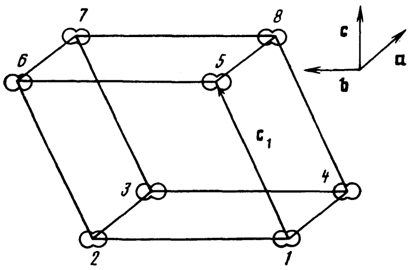

FIG. 5. Primitive unit cell in the Bravais lattice of the cyanogen groups in the orthorhombic phase. The **a**, **b**, and **c** axes are directed along the [110], [1$\bar{1}$0], and [001] axes of the cubic phase.

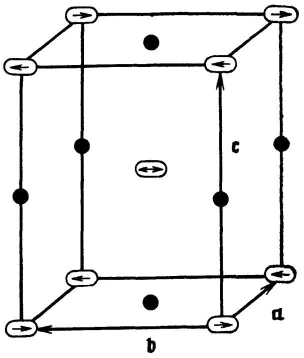

FIG. 6. Antiferroelectric ordering of the cyanogen groups in KCN below $T_{C3}=83$ K.

Lorentz method and it is again doubly degenerate; moreover, one of the states corresponds to our $|3\rangle$ state and the other is ferroelectric. Antiferroelectric ordering of the dipoles is predicted in Refs. 38–42 and it is attributed to elastic dipole interactions. The ordering reported in Ref. 38 is identical with that postulated above. In recent papers[39–42] the dipoles at the sites in the bcc orthorhombic cell are directed opposite to the central dipole.

6. CONCLUSIONS

The diagram technique for the Hubbard operators[4] can be used to consider also the orientational dynamics of the CN groups at phase transitions. If the treatment includes also the Hamiltonian of the interaction of the CN groups with phonons, it is also possible to consider lattice dynamics.

The above analysis applies specifically to KCN crystals, because the selection of the eigenfunctions of the energy levels (Table I) and of the coupling constants of Eq. (16) depends on the lattice parameter. The nature of the effective Hamiltonian of Eq. (14) or of the reduced variant of Eq. (17) of the representation of the wave functions of the CN group depends only on the symmetry of the problem which in this case is O_h. However, in the present analysis thset of the wave functions, and, consequently, of the thermodynamic potential is influenced also by the fact that the critical elastic modulus is C_{44}. Therefore, the off-diagonal, components of the strain tensor are used as the order parameter. However, there is also the possibility of a variant in which the critical elastic modulus is the difference C_{11}–C_{12}. In this case the diagonal components of the strain tensor act as the order diameter of the phase transition. This in turn affects significantly the selection of the wave functions and of the thermodynamic potential, as well as the phase diagram. However, this is outside the scope of the present paper.

We are deeply grateful to K. S. Aleksandrov and R. O. Zaĭdev for valuable critical comments and also to V. I. Zinenko for numerous valuable discussions.

APPENDIX A

The matrix of Eq. (15) splits into two independent blocks

$$T_1=\begin{pmatrix} \lambda & g_1u_{xy} & g_1u_{xz} & g_1u_{yz} \\ g_1u_{xy} & \lambda_6 & gu_{yz} & gu_{xz} \\ g_1u_{xz} & gu_{yz} & \lambda_7 & gu_{xy} \\ g_1u_{yz} & gu_{xz} & gu_{xy} & \lambda_8 \end{pmatrix},$$

$$T_2=\begin{pmatrix} \lambda_5 & g_2u_{yz} & g_2u_{xz} & g_2u_{xy} \\ g_2u_{yz} & \lambda_2 & \lambda u_{xy} & \lambda u_{xz} \\ g_2u_{xz} & \lambda u_{xy} & \lambda_3 & \lambda u_{yz} \\ g_2u_{xy} & \lambda u_{xz} & \lambda u_{yz} & \lambda_4 \end{pmatrix},$$

which apply to the representations $A_{1g}+F_{2g}$ and $A_{2u}+F_{1u}$, respectively. The eigenvalues for each of the matrices T_1 and T_2 are found from the equation

$$\mu^4+a_3\mu^3+a_2\mu^2+a_1\mu+a_0=0, \tag{A1}$$

where

$$a_3=-\operatorname{Tr} T,$$

$$\begin{aligned} a_2={}&T_{11}T_{22}+T_{11}T_{33}+T_{11}T_{44}+T_{22}T_{33}+T_{22}T_{44}\\ &+T_{33}T_{44}-T_{12}^2-T_{13}^2-T_{14}^2\\ &-T_{23}^2-T_{24}^2-T_{34}^2,\\ a_1={}&-T_{11}T_{22}T_{33}-T_{11}T_{22}T_{44}-T_{11}T_{33}T_{44}-T_{22}T_{33}T_{44}\\ &+T_{34}^2(T_{11}+T_{22})+T_{24}^2(T_{11}+T_{33})+T_{12}^2(T_{33}+T_{44})\\ &+T_{14}^2(T_{22}+T_{33})+T_{13}^2(T_{22}+T_{44})+T_{23}^2(T_{11}+T_{44})\\ &-2(T_{12}T_{14}T_{24}+T_{13}T_{14}T_{34}+T_{23}T_{24}T_{34}+T_{12}T_{13}T_{23}),\\ a_0={}&T_{14}^2T_{23}^2+T_{13}^2T_{24}^2+T_{12}^2T_{34}^2-2(T_{12}T_{13}T_{34}T_{24}+T_{12}T_{14}T_{23}T_{34}\\ &+T_{13}T_{14}T_{23}T_{24})-T_{34}^2T_{11}T_{22}-T_{24}^2T_{11}T_{33}-T_{23}^1T_{11}T_{44}\\ &-T_{14}^2T_{22}T_{33}-T_{13}^2T_{22}T_{44}. \end{aligned}$$

The relationships between the four roots of Eq. (A1) and its coefficients

$$\sum_{i=}^{4}\mu_i=-a_3,\quad \sum_{i<j}^{4}\mu_i\mu_j=a_2,$$

$$\sum_{i<j<k}^{4}\mu_i\mu_j\mu_k=-a_1,\quad \mu_1\mu_2\mu_3\mu_4=a_0,$$

obtained from the Vieta theorem allow us to deduce the following expressions:

$$\begin{gathered} \sum_{i=1}^{4}\mu_i^2=a_3^2-2a_2,\\ 2\sum_{i=1}^{4}\mu_i^3=a_3^3-3a_3\sum_{i=1}^{4}\mu_i^2-6a_1, \qquad \text{(A2)}\\ 3\sum_{i=1}^{4}\mu_i^4=a_3^4-4a_3\sum_{i=1}^{4}\mu_i^3+6\sum_{i<j}^{4}\mu_i^2\mu_j^2+12a_3a_1-24a_0. \end{gathered}$$

Expanding the expression

$$\ln \operatorname{Tr}\exp[-\beta(R_R+V)]=\ln\left\{\sum_{i=1}^{4}\sum_{r=1,2}\exp(-\beta\mu_i^{(r)})\right\}$$

in powers of $\beta\mu_i^{(r)}$, using the relationships given by (A2), and going back to the old variables $u_{\alpha\beta}$, we find from Eq. (14) that

$$\begin{aligned} F={}&{}^1/_2C_{11}(u_{xx}^2+u_{yy}^2+u_{zz}^2)+2C_{44}(u_{xy}^2+u_{yz}^2+u_{zx}^2)\\ &+C_{12}(u_{xx}u_{yy}+u_{yy}u_{zz}+u_{zz}u_{xx})\\ &+C_{112}[u_{xx}^2(u_{yy}+u_{zz})+u_{yy}^2(u_{xx}+u_{zz})\\ &+u_{zz}^2(u_{xx}+u_{yy})]+C_{166}[u_{xy}^2(u_{xx}+u_{yy})\\ &+u_{yz}^2(u_{yy}+u_{zz})+u_{zx}^2(u_{xx}+u_{zz})]\\ &+\gamma u_{xy}u_{yz}u_{zx}+C_{1111}(u_{xx}^4+u_{yy}^4+u_{zz}^4)\\ &+C_{1112}[u_{xx}^3(u_{yy}+u_{zz})+u_{yy}^3(u_{xx}+u_{zz})+u_{zz}^3(u_{xx}+u_{yy})]\\ &+C_{1122}[u_{xx}^2u_{yy}^2+u_{yy}^2u_{zz}^2\\ &+u_{zz}^2u_{xx}^2]+C_{1123}(u_{xx}+u_{yy}+u_{zz})u_{xx}u_{yy}u_{zz}\\ &+\frac{\alpha}{4}(u_{xy}^4+u_{yz}^4+u_{zx}^4)\\ &+{}^1/_2\delta(u_{xy}^2u_{xz}^2+u_{xy}^2u_{yz}^2+u_{xz}^2u_{yz}^2)+{}^1/_2C_1(u_{xx}+u_{yy}+u_{zz})\\ &+C_{111}(u_{xx}^3+u_{yy}^3+u_{zz}^3)\\ &+C_{123}u_{xx}u_{yy}u_{zz}+C_{1144}(u_{xx}^2u_{yz}^2+u_{yy}^2u_{xz}^2+u_{zz}^2u_{xy}^2)\\ &+C_{1155}[(u_{xy}^2+u_{yz}^2)u_{xx}^2\\ &+(u_{yz}^2+u_{xy}^2)u_{yy}^2+(u_{xz}^2+u_{yz}^2)u_{zz}^2]+C_{1244}[u_{xx}(u_{yy}+u_{zz})u_{yz}^2\\ &+u_{yy}(u_{xx}+u_{zz})u_{xz}^2\\ &+u_{zz}(u_{xx}+u_{yy})u_{xy}^2]+C_{1255}[u_{xx}(u_{yy}+u_{zz})(u_{xy}^2+u_{xz}^2)\\ &+u_{yy}(u_{xx}+u_{zz})(u_{xy}^2+u_{xz}^2)\\ &+u_{zz}(u_{xx}+u_{yy})(u_{xz}^2+u_{yz}^2)]\\ &+C_{1456}(u_{xx}+u_{yy}+u_{zz})u_{xy}u_{yz}u_{zx}, \end{aligned} \tag{A3}$$

where to within $\varepsilon_i=\beta(E_i^0-E_1^0)\ll 1$, $i=2,\dots,8$,

$$C_1=C_1^0-{}^1/_{64}\beta[\Delta_2(\gamma_2+2\gamma_3)+\Delta_3(\gamma_5+2\gamma_6)+2\gamma_4\Delta_4+2\gamma_1\Delta_1]$$

is the thermal expansion coefficient and

$$\begin{aligned} C_{11}={}&C_{11}^0-{}^1/_8\beta[\gamma_1^2+\gamma_3^2+\gamma_4^2+\gamma_6^2+2\gamma_2\gamma_3+2\gamma_5\gamma_6\\ &-{}^1/_8(\gamma_1+\gamma_2+\gamma_4+\gamma_5+2\gamma_3+2\gamma_6)^2]+{}^1/_{48}\beta^2\{3(\Delta_1+3\Delta_3)\cdot\\ &\times[\gamma_1^2+\gamma_6^2+2\gamma_5\gamma_6-(\gamma_1+\gamma_5+2\gamma_6)^2+3(\Delta_4+3\Delta_2)\cdot\\ &\times[\gamma_3^2+\gamma_4^2+2\gamma_2\gamma_3-(\gamma_2+\gamma_4+2\gamma_3)^2]\\ &+6(\gamma_1+\gamma_5+2\gamma_6)(2\Delta_3\gamma_6+\Delta_1\gamma_1+\Delta_3\gamma_5)\\ &+6(\gamma_2+\gamma_4+2\gamma_3)(2\Delta_2\gamma_3+\Delta_2\gamma_2+\Delta_4\gamma_4)\\ &+12\gamma_1\Delta_3(\gamma_5+2\gamma_6)+6\Delta_1\gamma_6(2\gamma_5+\gamma_6)\\ &+12\Delta_2\gamma_4(\gamma_2+2\gamma_3)+6\Delta_4\gamma_3(2\gamma_2+\gamma_3)\\ &+6\Delta_3\gamma_6(2\gamma_5+\gamma_6)+6\Delta_2\gamma_3(2\gamma_2+\gamma_3)\}\\ &-{}^1/_{64}\beta^2[(\Delta_1+\Delta_4+3\Delta_2+3\Delta_3)\\ &\times(\gamma_1^2+\gamma_3^2+\gamma_4^2+\gamma_6^2+2\gamma_2\gamma_3+2\gamma_5\gamma_6)\\ &+2(\gamma_1+\gamma_2+\gamma_4+\gamma_5+2\gamma_3+2\gamma_6)\\ &\times(\Delta_1\gamma_1+2\Delta_2\gamma_3+2\Delta_3\gamma_6+\Delta_4\gamma_4+\Delta_2\gamma_2+\Delta_3\gamma_5)],\\ C_{12}={}&C_{12}^0+(C_{11}-C_{11}^0)\\ &+{}^1/_{16}\beta^2[(\gamma_2-\gamma_3)^2(\Delta_2+\Delta_4)+(\gamma_5-\gamma_6)^2(\Delta_1+\Delta_3)],\\ C_{44}={}&C_{44}^0-{}^1/_4\beta(\lambda^2+g^2+g_1^2+g_2^2)\\ &+{}^1/_{32}\beta^2\{4g_1^2(\Delta_1+\Delta_3)+4g_2^2(\Delta_2+\Delta_4)\\ &-[\Delta_1+\Delta_4+3(\Delta_2+\Delta_3)](\lambda^2+g^2+g_1^2+g_2^2)\}, \end{aligned} \tag{A4}$$

where

$$\Delta_i = E^0_{i+1} - E_i^0.$$

Here, $C_{\alpha\beta}$, $C_{\alpha\beta\gamma}$, and $C_{\alpha\beta\gamma\delta}$ are the elastic moduli of the second, third, and fourth orders, respectively designated in accordance with the Voigt notation.[18] In the investigated range of temperatures we have $C_{\alpha\beta\gamma} > 0$ and $C_{\alpha\beta\gamma\delta} > 0$.

Using Eq. (A4), we can find the temperatures T_0 and T_0' at which the elastic moduli C_{44} and $C_{11}-C_{12}$ vanish, respectively:

$$T_0 = \frac{\lambda^2+g^2+g_1^2+g_2^2}{8C_{44}^0} + \Bigg\{ \left(\frac{\lambda^2+g^2+g_1^2+g_2^2}{8C_{44}^0} \right)^2$$

$$+ [(\Delta_1+\Delta_4+3(\Delta_2+\Delta_3)]$$

$$\times (\lambda^2+g^2+g_1^2+g_2^2) - 4g_1^2\Delta_3 - 4g_2^2(\Delta_2+\Delta_4)]/32C_{44}^0 \Bigg\}^{1/2}$$

$$\approx 270\ \mathrm{K},$$

$$T_0' = \left\{ \frac{(\gamma_2-\gamma_3)^2(\Delta_2+\Delta_4)+(\gamma_5-\gamma_6)(\Delta_1+\Delta_3)}{16(C_{11}^0-C_{12}^0)} \right\}^{1/2} \approx 20\ \mathrm{K}. \tag{A5}$$

APPENDIX B

The equations for an extremum of the thermodynamic potential of Eq. (17) are

$$\begin{aligned} &\tau x+\gamma yz+\alpha x^3+\delta x(y^2+z^2)=0, \\ &\tau y+\gamma xz+\alpha y^3+\delta y(x^2+z^2)=0, \\ &\tau z+\gamma xy+\alpha z^3+\delta z(x^2+y^2)=0, \end{aligned} \tag{B1}$$

where $\tau = 4C_{44}(\beta)$. The solutions of these equations can be classified in the following way[43]: (000), (x00), (xx0), (xxx), (xy0), (xxy), (xyz), where zeros denote $u_{\alpha\beta} = 0$, (xx0) means that $x = y$, $z = 0$, etc. [see Eq. (18)]. An analysis of these equations shows that, with the exception of isolated points in the space of the parameters of the thermodynamic potential of Eq. (17), we can expect the cubic (000), orthorhombic (x00), and rhombohedral (xxx) phases.

Substituting the solutions for the (xxx) and (x00) phases into Eq. (B1), we obtain the equations of state for the rhombohedral and orthorhombic phases, respectively:

$$\tau x+\gamma x^2+(\alpha+2\delta)x^3=0, \tag{B2}$$

$$\tau x+\alpha x^3=0. \tag{B3}$$

The transition temperatures can be found by comparing the thermodynamic potentials of the phases. The first-order transition from the cubic phase with $F = 0$ to the rhombohedral phase with $F = F(x_0)$, where in accordance with Eq. (B2), we have

$$x_0 = -\frac{\gamma}{2(\alpha+2\delta)}[1+(1-t)^{1/2}], \tag{B4}$$

$$t = \frac{4\tau(\alpha+2\delta)}{\gamma^2}, \tag{B5}$$

occurs when

$$\tau=\tau_1={}^2/_9\frac{\gamma^2}{\alpha+2\delta} > 0. \tag{B6}$$

In the range $\tau < 0$ the orthorhombic phase may be preferred if

$$-\frac{\tau^2}{4\alpha} \leqslant -\frac{3|\tau|}{2}x_0^2+\gamma x_0^3+{}^3/_4(\alpha+2\delta)x_0^4, \tag{B7}$$

where x is given by Eq. (B4). Consequently, Eq. (B7) can be reduced to the form

$$\gamma^2x_0^2-4\gamma|\tau|x_0 \leqslant 2\tau^2(\delta/\alpha-1). \tag{B8}$$

Since the right-hand side of Eq. (B8) is positive, the necessary condition for the existence of the orthorhombic phase is the inequality

$$\delta>\alpha. \tag{B9}$$

The inequality of Eq. (B8) can be rewritten in the form

$$\gamma x_0+2|\tau| \geqslant -|\tau|[2(1+\delta/\alpha)]^{1/2},$$

which readily yields the equation for the temperature of the transition from the rhombohedral to the orthorhombic phase:

$$\tau_2 = -{}^1/_4\frac{\gamma^2}{\alpha+2\delta}\frac{(2\xi-1)}{(\xi-1)^2}, \tag{B10}$$

where

$$\xi^2 = \frac{\alpha+2\delta}{2\alpha}.$$

Moreover, there is also an additional condition of stability of the thermodynamic phases at the minima:

$$F_{xx}>0, \quad \begin{vmatrix} F_{xx} & F_{xy} \\ F_{yx} & F_{yy} \end{vmatrix} > 0, \quad \begin{vmatrix} F_{xx} & F_{xy} & F_{xz} \\ F_{yx} & F_{yy} & F_{yz} \\ F_{zx} & F_{zy} & F_{zz} \end{vmatrix} > 0, \tag{B11}$$

where $F_{\alpha\beta} = \partial^2F/\partial x_\alpha \partial x_\beta$ and the quantities x_α are defined, as mentioned above, by the relationship (18). Substituting in Eq. (B11) the values $x_\alpha = (|\tau|/\alpha)^{1/2}$ and $y = z = 0$ for the orthorhombic phase, we readily obtain from the first inequality of Eq. (B11) the additional condition for the existence of the orthorhombic phase:

$$|\tau|>\alpha\gamma^2/(\delta-\alpha). \tag{B12}$$

[1] H. Tokunaga and T. Matsubara, Prog. Theor. Phys. **35**, 581 (1986).

[2] V. G. Vaks, *Introduction to the Microscopic Theory of Ferroelectrics* [in Russian], Nauka, Moscow (1973).

[3] J. Hubbard, Proc. R. Soc. London Ser. A **226**, 238 (1963).

[4] R. O. Zaĭtsev, Zh. Eksp. Teor. Fiz. **68**, 207 (1975) [Sov. Phys. JETP **41**, 100 (1975)].

[5] V. V. Val'kov and S. G. Ovchinnikov, Zh. Eksp. Teor. Fiz. **85**, 1666 (1983) [Sov. Phys. JETP **58**, 970 (1983)].

[6] L. D. Landau and E. M. Lifshitz, *The Classical Theory of Fields, 2nd ed.*, Pergamon Press, Oxford (1962), chap. 12.

[7] K. H. Michel and J. Naudts, J. Chem. Phys. **67**, 547 (1977).

[8] K. H. Michel and J. Naudts, J. Chem. Phys. **68**, 216 (1978).

[9] J. C. Raich and A. Hüller, J. Chem. Phys. **70**, 3669 (1979).

[10] B. De Raedt, K. Binder, and K. H. Michel, J. Chem. Phys. **75**, 2977 (1981).

[11] L. D. Landau and E. M. Lifshitz, *Theory of Elasticity, 2nd ed.*, Pergamon Press, Oxford (1970).

[12] R. M. Lynden-Bell, I. R. McDonald, and M. L. Klein, Mol. Phys. **48**, 1093 (1983).
[13] D. E. Williams, J. Chem. Phys. **47**, 4680 (1967).
[14] M. P. Tosi, Solid State Phys. **16**, 1 (1964).
[15] S. Haussühl, Solid State Commun. **13**, 147 (1973).
[16] J. P. Elliot and P. G. Dawper, *Symmetry in Physics, Vol. 1*, Macmillan, London (1979), chap. 5.
[17] W. Krasser, U. Buchenau, and S. Haussühl, Solid State Commun. **18**, 287 (1976).
[18] L. K. Zarembo and V. A. Krasil'nikov, *Introduction to Nonlinear Acoustics* [in Russian], Nauka, Moscow (1966), chap. 3.
N. G. Parsonage and L. A. K. Staveley, *Disorder in Crystals*, Clarendon Press, Oxford (1979), chap. 7.
[20] G. S. Parry, Acta Crystallogr. **15**, 596 (1962).
[21] H. Suga, T. Matsuo, and S. Seki, Bull. Chem. Soc. Jpn. **38**, 1115 (1965).
[22] A. Cimino, G. S. Parry, and A. R. Ubbelohde, Proc. R. Soc. London Ser. A **252**, 445 (1959).
[23] C. W. F. T. Pistorius, J. B. Clark, and E. Rapoport, J. Chem. Phys. **48**, 5123 (1968).
[24] M. Atoji, J. Chem. Phys. **54**, 3514 (1971).
[25] D. E. O'Reilly, E. M. Peterson, C. E. Scheie, and P. K. Kadaba, J. Chem. Phys. **58**, 3018 (1973).
[26] W. Rehwald, J. R. Sandercock, and M. Rossinelli, Phys. Status Solidi A **42**, 699 (1977)
[27] D. Kh. Blat and V. I. Zinenko, Zh. Eksp. Teor. Fiz. **79**, 974 (1980) [Sov. Phys. JETP **52**, 495 (1980)].
[28] E. Ohno and K. Yoshimitsu, Prog. Theor. Phys. Suppl. No. 80, 180 (1984).
[29] E. Ohno, J. Phys. Soc. Jpn. **56**, 4414 (1987).
[30] A. F. Sadreev and Yu. V. Sukhinin, Preprint No. 513-F [in Russian], Institute of Physics, Siberian Division of the USSR Academy of Sciences, Krasnoyarsk.
[31] D. L. Price, J. M. Rowe, J. J. Rush, E. Prince, D. G. Hinks, and S. Susman, J. Chem. Phys. **56**, 3697 (1972).
[32] J. P. von der Weid, L. C. Scavarda do Carmo, R. R. Do Santos, *et al.*, J. Phys. (Paris) **37**, Colloq. 7, C7-291 (1976).
[33] J. M. Rowe, J. J. Rush, and E. Prince, J. Chem. Phys. **66**, 5147 (1977).
[34] T. Matsuo, H. Suga, and S. Seki, Bull. Chem. Soc. Jpn. **41**, 583 (1968).
[35] R. Blinc and B. Žekš, *Soft Modes in Ferroelectrics and Antiferroelectrics*, North-Holland, Amsterdam (1974), chap. 5.
[36] W. Dultz, Solid State Commun. **15**, 595 (1974).
[37] T. Niemeyer, Physica (Utrecht) **57**, 281 (1972).
[38] R. R. Dos Santos, B. Koiller, J. P. von der Weid, *et al.*, J. Phys. C **11**, 4557 (1978).
[39] E. Ohno, J. Phys. Soc. Jpn. **56**, 4414 (1987).
[40] R. Pirc and I. Vilfan, Solid State Commun. **39**, 181 (1981).
[41] B. Koiller, M. A. Davidovich, L. C. Scavarda do Carmo, and F. Lüty, Phys. Rev. B **29**, 3586 (1984).
[42] H. T. Stokes and D. M. Hatch, Phys. Rev. B **30**, 3485 (1984).
[43] Yu. A. Izyumov and V. N. Syromyatnikov, *Phase Transitions and Symmetry of Crystals* [in Russian], Nauka, Moscow (1984), chap. 5.

Translated by A. Tybulewicz